Cancer Therapy: Preclinical

Clinical Cancer Research

New Molecular and Biological Mechanism of Antitumor Activities of KW-2478, a Novel Nonansamycin Heat Shock Protein 90 Inhibitor, in Multiple Myeloma Cells

Takayuki Nakashima[1], Toshihiko Ishii[1], Hisashi Tagaya[1], Toshihiro Seike[1], Hiroshi Nakagawa[1], Yutaka Kanda[1], Shiro Akinaga[2], Shiro Soga[1], and Yukimasa Shiotsu[1]

Abstract

Purpose: The heat shock protein 90 (Hsp90) plays an important role in chaperoning oncogenic client proteins in multiple myeloma (MM) cells, and several Hsp90 inhibitors have shown antitumor activities both *in vitro* and *in vivo*. However the precise mechanism of action of Hsp90 inhibitor in MM has not been fully elucidated.

Experimental Design: We evaluated the antitumor activities of KW-2478, a nonansamycin Hsp90 inhibitor, in MM cells with various chromosomal translocations of immunoglobulin heavy chain (IgH) loci both *in vitro* and *in vivo*.

Results: Our studies revealed that exposure of KW-2478 to MM cells resulted in growth inhibition and apoptosis, which were associated with degradation of well-known client proteins as well as a decrease in IgH translocation products (FGFR3, c-Maf, and cyclin D1), and FGFR3 was shown to be a new client protein of Hsp90 chaperon complex. In addition, KW-2478 depleted the Hsp90 client Cdk9, a transcriptional kinase, and the phosphorylated 4E-BP1, a translational inhibitor. Both inhibitory effects of KW-2478 on such transcriptional and translational pathways were shown to reduce c-Maf and cyclin D1 expression. In NCI-H929 s.c. inoculated model, KW-2478 showed a significant suppression of tumor growth and induced the degradation of client proteins in tumors. Furthermore, in a novel orthotopic MM model of i.v. inoculated OPM-2/green fluorescent protein, KW-2478 showed a significant reduction of both serum M protein and MM tumor burden in the bone marrow.

Conclusions: These results suggest that targeting such diverse pathways by KW-2478 could be a promising strategy for the treatment of MM with various cytogenetic abnormalities. *Clin Cancer Res; 16(10); 2792-802. ©2010 AACR.*

Multiple myeloma (MM) is a B-cell malignancy characterized by complex cytogenetic abnormalities. The chromosomal translocations involving the immunoglobulin heavy chain (IgH) locus and different chromosomal partners occur in ~60% of MM patients. Such genomic instability and complexities might explain MM cell resistance to existing therapies (1, 2). Recent studies have revealed that IgH translocations involve several recurrent chromosomal loci, including 11q13 (*cyclin D1*), 6p21 (*cyclin D3*), 4p16 (*FGFR3* and *MMSET*), 16q23 (*c-MAF*), and 20q11 (*MAFB*; refs. 2, 3).

Authors' Affiliations: [1]Research Division, Kyowa Hakko Kirin Co., Ltd., Shizuoka, Japan and [2]Development Division, Kyowa Hakko Kirin Co., Ltd., Tokyo, Japan

Note: Supplementary data for this article are available at Clinical Cancer Research Online (http://clincancerres.aacrjournals.org/).

Corresponding Author: Yukimasa Shiotsu, Research Division, Kyowa Hakko Kirin Co., Ltd., 1188 Shimotogari, Nagaizumi-cho, Sunto-gun, Shizuoka 411-8731, Japan. Phone: 81-55-989-2004; Fax: 81-55-986-7430; E-mail: yukimasa.shiotsu@kyowa-kirin.co.jp.

doi: 10.1158/1078-0432.CCR-09-3112

Heat shock protein 90 (Hsp90) is a ubiquitously expressed molecular chaperone and assists the correct conformation, stabilization, and activation of client proteins, most of which are responsible for tumor development and progression. Given the critical roles played by Hsp90 and its client proteins in oncogenesis, targeting Hsp90 has emerged as a possible strategy for treatment of advanced cancers, including MM (4, 5).

Several groups have reported that the natural products geldanamycin, radicicol, and their derivatives are shown to bind and inhibit the function of Hsp90 chaperon complex, leading to degradation of Hsp90 client proteins by the ubiquitin-proteasome pathway (6–9). The discovery that geldanamycin and radicicol bind to Hsp90 and possess potent antitumor activities by the destabilization of oncogenic proteins drew interest in the potential use of these agents as new anticancer drugs (9, 10). A geldanamycin derivative, 17-AAG, showed antitumor activity in various human tumor xenograft models (11, 12) and is the first anticancer drug of its class to have entered clinical trials (13, 14). It is also reported that 17-AAG inhibits proliferation and survival of MM cells, associated with suppression of cell

Translational Relevance

KW-2478 is a novel heat shock protein 90 (Hsp90) inhibitor of nonnatural product that overcomes limitations of 17-allylamino-17-demethoxygeldanamycin (17-AAG), such as low water solubility and hepatotoxicity. In this study, we show that KW-2478 has more favorable pharmacologic activities than 17-AAG in animal studies. In addition, we reveal that FGFR3 is a new Hsp90 client protein and new mechanism of actions of Hsp90 inhibitor, KW-2478, in MM cells with various chromosomal translocation. Exposure of KW-2478 to MM cells not only depleted the well-known Hsp90 client proteins but also immunoglobulin heavy chain translocation products (cyclin D1 and c-Maf). We confirmed that the depletion of Cdk9 and the dephosphorylation of 4E-BP1 were associated with downregulation of c-Maf and cyclin D1. These findings indicate that targeting such diverse pathways by continuous drug exposure could be a promising strategy for the treatment of MM, characterized by complex cytogenetic abnormalities.

surface expression of interleukin-6R, insulin-like growth factor (IGF-IRβ), and their downstream signaling molecules, including the phosphoinositide 3-kinase/Akt and Ras/Raf/mitogen-activated protein kinase pathways (15, 16). Furthermore, 17-AAG exhibited clinical activity in patients with relapsed and refractory MM in Phase I clinical trials (17, 18). IPI-504 and 17-dimethylaminoethylamino-17-demethoxy-geldanamycin, the other geldanamycin analogues with improved solubility, have also been investigated in clinical trials (13, 14).

However, these geldanamycin analogues have limitations in clinical use, because of their hepatotoxicity, difficulties in formulation, variable pharmacokinetics, polymorphic metabolism by CYP3A4, and NQO1/DT diaphorase enzymes (19, 20). Despite these limitations of first generation Hsp90 inhibitors, the findings in clinical trials have encouraged further discovery of novel Hsp90 inhibitors. Recently, some novel Hsp90 inhibitors (e.g., NVP-AUY922, SNX-5422, and BIIB021) are discovered and already undergoing clinical trials (21, 22). Here, we report a new molecular and pharmacologic mechanism of antitumor activities using neither ansamysin nor radicicol Hsp90 inhibitor, KW-2478, in human MM cells having various IgH translocations.

Materials and Methods

Reagents and antibodies. KW-2478, 2-{2-ethyl-3,5-dihydroxy-6-[3-methoxy-4-(2-morpholin-4-ylethoxy)-benzoyl]phenyl}-*N*,*N*-bis(2-methoxyethyl)acetamide monohydrochloride, and biotinylated radicicol (bRD; ref. 23) were synthesized in house. KW-2478 with a highly water soluble profile (>30 mg/mL) was dissolved in saline. 17-AAG was obtained from Funakoshi. IGF-IRβ, c-Raf-1, and c-Maf antibodies were obtained from Santa Cruz Biotechnology. FGFR3 and β-actin antibodies were obtained from Sigma-Aldrich. Poly(ADPribose) polymerase (PARP) antibody was obtained from Trevigen. Cyclin D1, phosphorylated extracellular signal-regulated kinase 1/2 (Erk1/2; Thr^{202}/Tyr^{204}), Cdk7, Cdk9, phosphorylated Cdk9 (Thr^{186}), Akt, phosphorylated Akt (Ser^{473}), 4E-BP1, and phosphorylated 4E-BP1 ($Thr^{37/46}$) antibodies were obtained from Cell Signaling Technology. Erk2 antibody was obtained from Upstate Group, Inc. Horseradish peroxidase (HRP)–conjugated antimouse IgG and HRP-conjugated antirabbit IgG were obtained from GE Healthcare Bio-Sciences. Hsp70 antibody was obtained from Assay Designs.

Hsp90 binding assay. Human Hsp90α (Assay Designs) solution (0.5 μg/mL) was fixed on 96-well plates, followed by blocking with TBS containing 1% bovine serum albumin. The drug solutions were added to the wells, and bRD was added to a concentration of 0.1 μmol/L. After removal of solution, poly-HRP streptavidin solution (Pierce Biotechnology) diluted with poly-HRP dilution buffer (Pierce Biotechnology) was added to the wells. After removal of solution, equal volumes of TMB peroxidase substrate (Bethyl Laboratories) and peroxidase solution B (Bethyl Laboratories) were added to the wells. To stop the HRP reaction, 2 mol/L H_2SO_4 were added, followed by measurement of absorbance at 450 nm using a microplate spectrophotometer.

Cell culture and* in vitro *growth inhibitory profile of KW-2478. OPM-2/green fluorescent protein (GFP) cells were obtained from AntiCancer, Inc. KMS-11 cells were kindly provided by Dr. Otsuki (Kawasaki Medical School). OPM-2/GFP and KMS-11 cells were cultured according to instructions and authenticated in this paper. Other cell lines were recently obtained from American Type Culture Collection or Deutsche Sammlung von Mikroorganismen und Zellkulturen and cultured according to instructions.

The cells were plated into 96-well plates and treated with KW-2478. After 72 hours of cultivation, cell viability was determined using Cell Proliferation Reagent WST-1 (Roche Diagnostics). WST reagent was added to the wells, followed by incubation for 4 hours at 37°C. After that, the absorbance at 450 nm with reference at 650 nm was measured with a microplate spectrophotometer.

To examine time dependency of antiproliferative activity of KW-2478, the cells were plated into 96-well V-bottomed plates and treated with KW-2478. After 0 hour and at intervals from 3 to 72 hours at 37°C, the supernatant was aspirated. After drug-free medium was added to the wells, the supernatant was aspirated again. Finally, drug-free medium was added to the wells, and the plates were further incubated for the remainder of the 72-hour period, followed by measurement of cell viability.

Western blot analysis. Protein extraction and Western blot analysis were done as described previously (24).

Real-time PCR. The cells were treated with KW-2478, and total RNA was extracted using an RNeasy Plus Mini kit (QIAGEN) and QIA shuredder (QIAGEN). cDNA was synthesized using a Superscript VILO cDNA synthesis kit (Invitrogen). SYBR Green real-time PCR (Applied Biosystems) was done on cDNA prepared from the cells. Primer sequences were designed for each mRNA: c-Maf, forward 5′-TTCCTTTTGGCTTGGAAATG-3′ and reverse 5′-GTGCATTGGGAGGTTGAAGT-3′; cyclin D1, forward 5′-AACTACCTGGACCGCTTCCT-3′ and reverse 5′-CCACTTGAGCTTGTTCACCA-3′; and glyceraldehyde-3-phosphate dehydrogenase, forward 5′-GATGACATCAAGAAGGTGGTGA-3′ and reverse 5′-TTCGTTGTCATACCAGGAAATG-3′. Thermal cycling conditions were 10 minutes at 95°C, 35 cycles at 95°C for 15 seconds, followed by 1 minute at 60°C. Data analysis was completed using the ABI PRISM 7900HT Sequence Detection software (Applied Biosystems). Real-time PCR was done in duplicate, and glyceraldehyde-3-phosphate dehydrogenase was used for normalization.

Antitumor activity in NCI-H929 xenograft model. Severe combined immunodeficient (SCID) mice (CLEA Japan) were i.p. injected with anti-asialo GM1 antibody (Wako Pure Chemical Industries). The next day, all mice were s.c. inoculated with NCI-H929 cells (ref. 25; 1×10^7) suspended in PBS containing 50% of Matrigel (BD Biosciences). After 10 days, tumor volume was measured using the Antitumor Test System II (Human Life), a computer-operated system including software and instruments. SCID mice with tumors (190 to 290 mm^3) were selected. After randomly grouping, saline (vehicle) or KW-2478 was i.v. given to mice once or twice daily for 5 days. 17-AAG was dissolved as described before (11) and i.v. given to mice. Tumor volume was calculated by the Antitumor Test System II as follows: tumor volume = DL × DS × DS × 1/2 (DL, long diameter; DS, short diameter). Fourteen days after the initial administration, blood samples of each mouse were obtained, followed by measurement of serum M protein (Igκ chain) with Human Kappa-b&f ELISA Quantitation kit (Bethyl Laboratories). The statistical analysis was done using SAS software (SAS Institute, Inc.).

Pharmacodynamic study in NCI-H929 xenograft. SCID mice with s.c. NCI-H929 tumors (310 to 550 mm^3) were prepared as described above. KW-2478 was i.v. given to mice once daily for 5 days. One to 24 hours after the fifth administration, tumor samples were collected and homogenized in the lysis buffer (24). After centrifugation, tumor lysates were obtained and protein concentrations of each sample were measured with a protein assay kit (Bio-Rad Laboratories). Western blot was done as described previously (24).

Antitumor activity in OPM-2/GFP orthotopic model. The antitumor activity of KW-2478 was evaluated on GFP-overexpressing OPM-2/GFP tumors growing in bone marrow by whole-body imaging of GFP. Cyclophosphamide (3 mg per mouse, Shionogi) was i.p. given to SCID mice once daily for 2 days. The next day (day 0), 40 mice were i.v. inoculated with OPM-2/GFP cells (1×10^7) suspended in PBS. Twenty days after the inoculation (day 20), blood samples of each mouse were obtained, followed by measurement of serum M protein (Igλ chain; ref. 26) concentration with Human Lambda-b&f ELISA Quantitation kit (Bethyl Laboratories). Ten mice, which M protein concentrations were nearest to the mean of all mice, were divided into two groups ($n = 5$) on day 24. KW-2478 (100 mg/kg) was i.v. given to the mice twice daily for 5 days. To measure serum M protein concentration after the dosing on days 31, 38, and 45, blood samples were obtained from each mouse, followed by measurement of serum M protein concentrations. To evaluate the antitumor activity, on day 48 the fluorescence of GFP in the tumor-bearing mice was measured. The mice were anesthetized, and the fur was shaved completely. Whole-body fluorescence images of the mice were measured from the dorsal angle with an AQUACOSMOS/Macro Fluorescence System (Hamamatsu Photonics) consisting of a xenon lamp, CCD camera, lenses, and image processing software (AquaCosmos, Hamamatsu Photonics).

Results

Chemical structure, Hsp90 binding activity, and antiproliferative activity of KW-2478. The chemical structure of KW-2478, a novel Hsp90 inhibitor, is shown in Fig. 1A. KW-2478 was newly discovered by a unique lead optimization strategy, including microbial screening, X-ray crystallography, cell-based screening, and *in vivo* models. The binding activity of KW-2478 to Hsp90 was examined by a colorimetric ELISA using the immobilized human Hsp90α and bRD (Fig. 1B). KW-2478 inhibited the binding of bRD to Hsp90α, in accordance with increasing concentration of the compound, giving an IC_{50} value of 3.8 nmol/L. The antiproliferative activities of KW-2478 against cultured human MM and non–Hodgkin's lymphoma were evaluated. Fifty percent of growth inhibitory concentration values of KW-2478 against human MM cells, OPM-2/GFP, KMS-11, RPMI 8226, and NCI-H929, were 0.30, 0.34, 0.39, and 0.12 μmol/L, respectively. Those against human non–Hodgkin's lymphoma cells, Raji, SR, and SC-1, were 0.36, 0.098, and 0.33 μmol/L, respectively. KW-2478 showed potent and broad growth inhibitory activities against various human hematologic tumor cells.

Expression of FGFR3, c-Maf, and cyclin D1 proteins in MM cells. The expression levels of Hsp90 client proteins [IGF-IRβ (15, 27) and c-Raf-1 (7)] and the translocation products of IgH locus (FGFR3, cyclin D1, and c-Maf) in MM cell lines were examined (Fig. 2A). Western blot analysis showed different levels of FGFR3 in the cell lines with t(4;14) translocation, indicating FGFR3 overexpression in KMS-11, OPM-2/GFP, and NCI-H929 cells. As previously reported, KMS-11 and OPM-2, a parental cell line of OPM-2/GFP, are associated with highly elevated FGFR3, whereas NCI-H929 has relatively low level of FGFR3 (28). RPMI 8226 displayed a high level of c-Maf protein associated with t(16;22), a complex chromosomal rearrangement resulting in overexpression of c-Maf (29, 30). In addition,

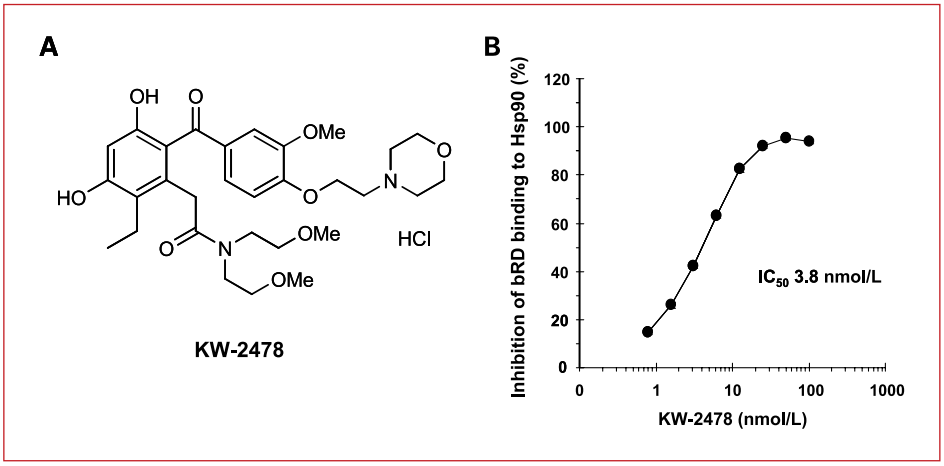

Fig. 1. Chemical structure and Hsp90 binding activity of KW-2478. A, chemical structure of KW-2478. B, the binding affinity of KW-2478 was examined using immobilized human Hsp90α and a biotinylated Hsp90 binding agent (bRD). Points, mean (n = 3).

c-Maf expression was detected in KMS-11 with t(14;16) as well as OPM-2/GFP and NCI-H929 without t(14;16; ref. 30). Regarding cyclin D1, the overexpression was detected in U266 with t(11;14), which caused aberrant expression (30).

Effects of KW-2478 on the Hsp90 client proteins and the translocation products of IgH loci in MM cells. The effect of KW-2478 was examined in t(4;14)-positive MM cell lines, OPM-2/GFP and NCI-H929, which express actively mutated FGFR3 (K650E) and wild-type FGFR3 proteins, respectively (Fig. 2B; ref. 28). The treatment of NCI-H929 and OPM-2/GFP cells with KW-2478 for 24 hours resulted in degradation of FGFR3 as well as known Hsp90 client proteins, IGF-IRβ and c-Raf-1. KW-2478 also reduced the level of phosphorylated Erk1/2, whereas it did not affect the expression level of β-actin protein, indicating that the reduction was the consequence of degradation of the upstream molecules, IGF-IRβ, c-Raf-1, and FGFR3. In OPM-2/GFP and NCI-H929 cells, treatment with KW-2478 caused cleavages of PARP, a substrate of caspase-3, this suggested apoptosis induction. Further immunoblot analysis confirmed that KW-2478 activated the intrinsic apoptotic pathway (Supplementary Fig. S1). Next, the effects of KW-2478 on c-Maf and cyclin D1 proteins were examined (Fig. 2B). The treatment of RPMI 8226 with KW-2478 for 24 hours resulted in depletion of c-Maf protein as well as IGF-IRβ and c-Raf-1. In U266 cells, treatment with KW-2478 for 24 hours resulted in depletion of cyclin D1 protein and cleavage of PARP, indicating caspase-dependent apoptosis. In addition, exposure of MM cells to KW-2478 resulted in an extensive induction of Hsp70, indicating that Hsp70 induction could be a biomarker for Hsp90 inhibition.

Time dependency of antiproliferative activity of KW-2478. The relationship between the antiproliferative activity of KW-2478 and treatment duration was examined with OPM-2/GFP and NCI-H929 cells (Fig. 3). The cells were treated with the increasing concentrations of KW-2478 at intervals from 30 hours to 72 hours and further incubated in drug-free medium for the remainder of the 72-hour period, followed by measuring viable cell number. When the cells were treated with KW-2478 for <6 hours, the antiproliferative activity of KW-2478 was limited with IC_{80} values of >30 μmol/L. However, when cells were treated for 12 hours or longer, the antiproliferative activity was more potent as the exposure time was longer, with IC_{80} values of 3.3 μmol/L or less. These results show that the antiproliferative activity of KW-2478 is time dependent, and consecutive drug exposure for at least 12 hours might be necessary to exert potent antitumor activity.

New mechanism of action by KW-2478 to downregulate the translocation products of IgH loci in MM cells. As of this writing, there is no report that shows that FGFR3, c-Maf, and cyclin D1 proteins are clients of Hsp90 chaperon complex. Because several receptor tyrosine kinases are reported to be Hsp90 client protein, we assessed if FGFR3 would be the Hsp90 client protein. In OPM-2/GFP cells, the depletion of FGFR3 protein was detected as early as 6 hours after the treatment with KW-2478 (3 μmol/L) without affecting other protein levels at this time point (Fig. 4A). The depletion of FGFR3 by KW-2478 over 6 hours of treatment was due to its degradation through proteasome pathway, because the level of FGFR3 in NP40-insoluble fraction was clearly restored by cotreatment of the proteasome inhibitor MG-132, like c-Raf protein (Supplementary Fig. S2). In addition, we confirmed the interaction of FGFR3 and Hsp90 assessed by the immunoprecipitation analysis with FGFR3 antibody and Western blotting with Hsp90 antibody (Supplementary Fig. S3). These results indicate that FGFR3 is a client protein stabilized by Hsp90 chaperon complex. In the same way, we examined the interaction of c-Maf and Hsp90 in RPMI 8226 cells, although the coimmunoprecipitation was not detected (data not shown), which suggested that c-Maf could not be an Hsp90 client protein.

To examine the molecular basis of depletion of c-Maf and cyclin D1 proteins by KW-2478, we examined the effects on transcriptional and translational regulations of these genes, focusing on the transcriptional Cdks, such as Cdk7 and Cdk9 (the latter was reported to be an

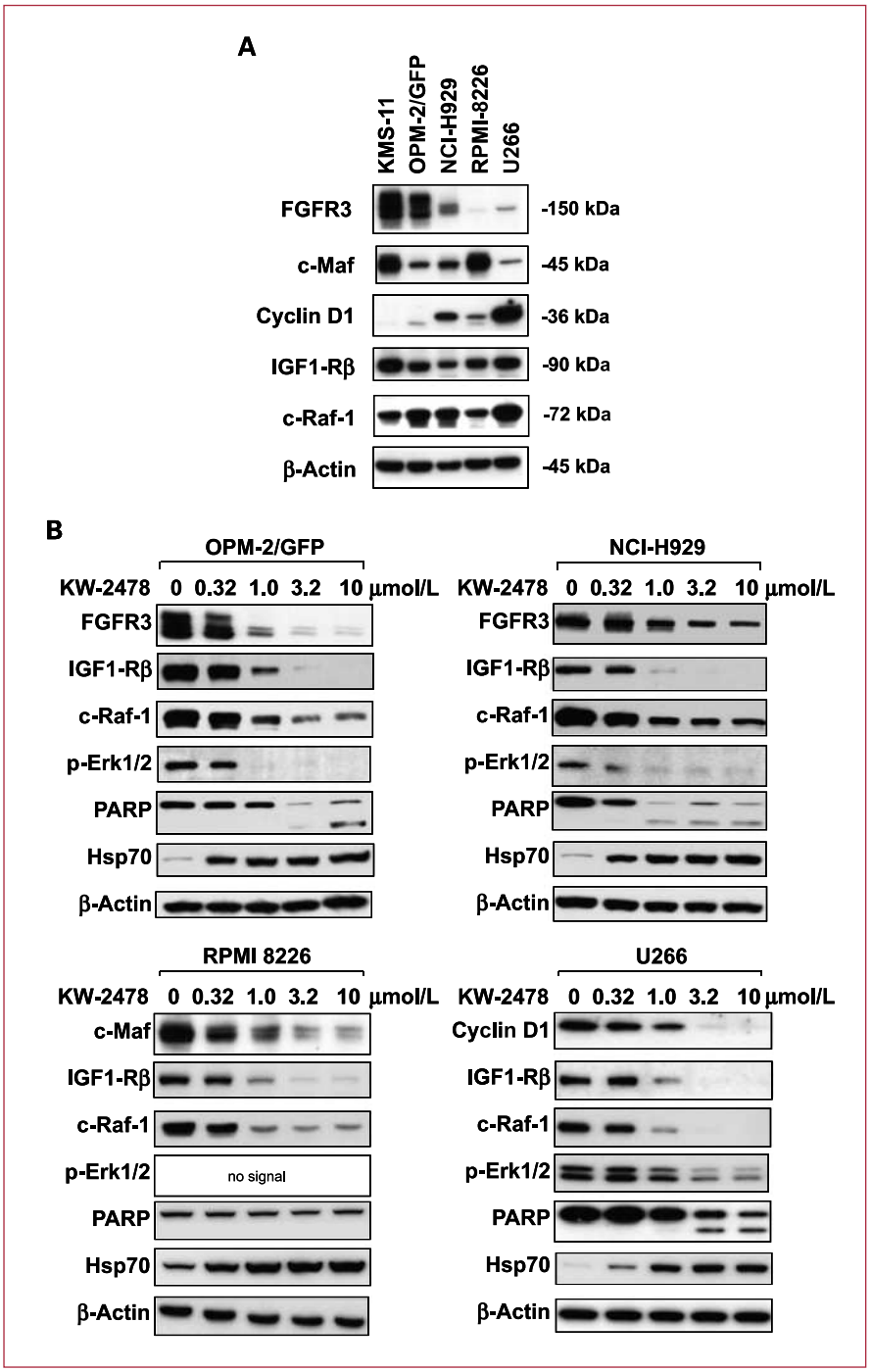

Fig. 2. Effects of KW-2478 on FGFR3, c-Maf, and cyclin D1 proteins. A, the expression levels of Hsp90 client proteins (IGF-1Rβ and c-Raf-1) and the translocation products (FGFR3, c-Maf, and cyclin D1) of IgH loci in MM cells (KMS-11, OPM-2/GFP, NCI-H929, RPMI 8226, and U266) were examined by Western blot analysis. β-Actin level was used as a loading control. B, OPM-2/GFP, NCI-H929, RPMI 8226, and U266 cells were treated with increasing concentrations of KW-2478 for 24 h. Total cell lysates were analyzed by Western blot analysis with FGFR3, c-Maf, cyclin D1, IGF-1Rβ, c-Raf-1, phosphorylated Erk1/2 (Thr^{202}/Tyr^{204}; p-Erk1/2), PARP, Hsp70, and β-actin antibodies.

Hsp90 client protein; ref. 31), and 4E-BP1, a translational inhibitor (32). The phosphorylated forms of Cdk9 and 4E-BP1 proteins were detected in all MM cell lines, suggesting that Cdk9 and 4E-BP1 might play critical roles in expression of the translocation products of IgH loci (Supplementary Fig. S4). In RPMI 8226 and U266 cells, the decrease of c-Maf and cyclin D1 proteins was detected 12 hours after the treatment with KW-2478 (3 μmol/L), which was associated with the downregulation of Cdk9, Akt, and the dephosphorylation of 4E-BP1 (Fig. 4A). This suggested that downregulations of both Cdk9-mediated transcriptional and 4E-BP1-regulated translational pathways could be the cause for the decreases of c-Maf and cyclin D1 proteins. To examine the inhibitory effect of KW-2478 on the transcription, the levels of c-Maf and cyclin D1 mRNAs were investigated by real-time PCR. As shown in Fig. 4B,

KW-2478 induced the downregulation of these mRNAs after 3 hours of treatment. These findings indicated that KW-2478 inhibited the transcription of c-Maf and cyclin D1 genes by mainly suppressing the function of Cdk9. Moreover, we confirmed that the Cdk9 inhibitor flavopiridol induced the downregulation of cyclin D1 and c-Maf proteins without any effect on β-actin level (Supplementary Fig. S5).

In vivo *antitumor activities of KW-2478 in NCI-H929 tumors s.c. inoculated in SCID mice.* The *in vivo* antitumor activity of KW-2478 was examined in a SCID mouse model bearing human MM xenograft. In this model, NCI-H929 cells were s.c. inoculated into SCID mice and KW-2478 was i.v. given once daily for 5 days at doses of 25 to 200 mg/kg. Our previous studies had shown that a single dosing of KW-2478 at 25 mg/kg induced the elevation of Hsp70 protein in NCI-H929 tumors (data not shown). As shown in Fig. 5A, KW-2478 showed significant suppression of tumor growth at doses of 25 to 200 mg/kg without loss of body weight. Furthermore, we compared the antitumor activity of KW-2478 and 17-AAG in the same model. Whereas KW-2478 was well tolerated and exhibited greater pharmacologic property at 25 to 100 mg/kg (twice daily for 5 days; Fig. 5B), 17-AAG at 40 mg/kg only showed that significant suppression of tumor growth and treatment of mice at 40 mg/kg or greater resulted in severe loss of body weight and several animal deaths.

In vivo *Hsp90 inhibitory activities of KW-2478 in NCI-H929 tumors.* To confirm Hsp90 inhibitory activities of KW-2478 *in vivo*, levels of IGF-IRβ, c-Raf-1, phosphorylated Erk1/2, Cdk9, and Hsp70 in tumors were examined after administration of KW-2478 (Fig. 5C). In this study, KW-2478 (100 mg/kg) was i.v. given to mice once daily for 5 days and tumor samples were collected at 1 to 24 hours after the final administration. At this dose, pronounced decreases in IGF-IRβ, c-Raf-1, Cdk9, and phosphorylated Erk1/2 levels were observed, indicating that the dosing of KW-2478 induced degradation of the Hsp90 client proteins and dephosphorylated Erk1/2 proteins in tumors, similarly to the *in vitro* cellular effects of KW-2478 (Fig. 5C). These results showed that antitumor activities of KW-2478 were also caused by an inhibition of Hsp90 chaperone function in tumors after 5 days of consecutive administration.

In vivo *antitumor activity of KW-2478 in OPM-2/GFP i.v. inoculated mouse model.* To investigate the antitumor activity of KW-2478 in a bone marrow environment, we developed a novel orthotopic mouse model in which multi-MM lesions were developed after i.v. inoculation of OPM-2/GFP cells. In this model, whole-body fluorescence imaging (WFI) was used to monitor the inhibition of *in vivo* growth of MM tumors noninvasively after KW-2478 administration. Comprehensive monitoring of growth of metastatic lesions was successfully captured by WFI in this model. Most of the mice inoculated i.v. with OPM-2/GFP cells were found to develop multiple skeletal lesions, which were mainly localized in bone marrow spaces of spine and leg bones (tibia and femur), resulting in frequent development of paralysis (data not shown). Besides these skeletal lesions, MM tumors were also observed in liver and lung as nondominant lesions.

In this orthotopic model, the antitumor activity of KW-2478 was evaluated as described in Fig. 6A. SCID mice were i.v. inoculated with OPM-2/GFP cells, a serum sample was obtained from each mouse, and the concentration of serum M protein (Igλ chain) was measured after 20 days. Ten mice, for which serum M protein concentrations were nearest to the mean value of all serum samples, were selected and divided into two groups (n = 5). After 24 days, KW-2478 (100 mg/kg) was given i.v. twice daily for 5 days. On day 48 (20 days after the final administration), the growth of MM tumors was observed by WFI (Fig. 6B). In control mice, the fluorescence of GFP was detected mainly along the spine and in the knee (femur and/or tibia), indicating that the MM cells grew preferentially in the bone marrow environment. The intensity of

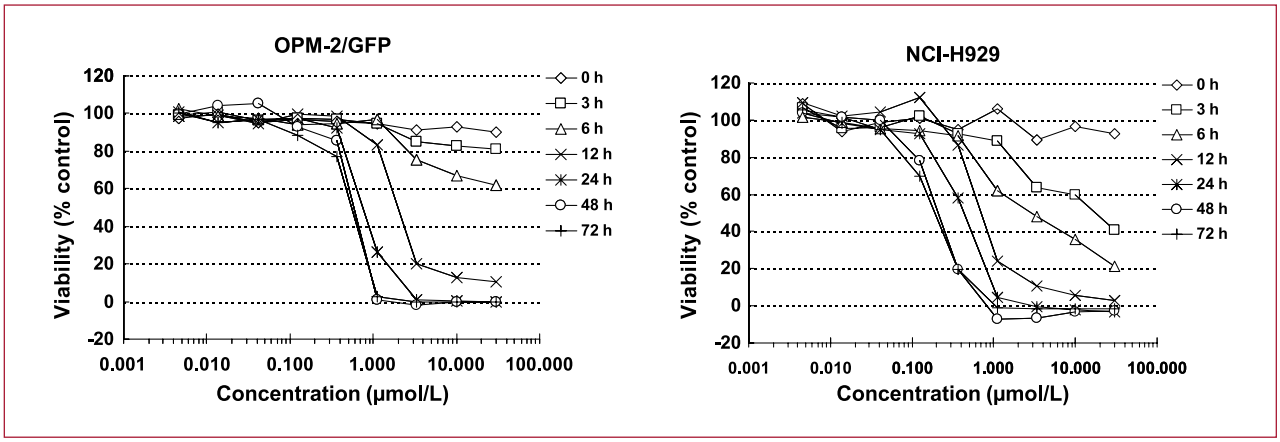

Fig. 3. Time dependency of antiproliferative activity of KW-2478. OPM-2/GFP and NCI-H929 cells were treated with increasing concentrations of KW-2478 for 0, 3, 6, 12, 24, 48, and 72 h and further incubated in drug-free medium for the remainder of the 72-h period, followed by measuring viable cell number. Points, mean (n = 3).

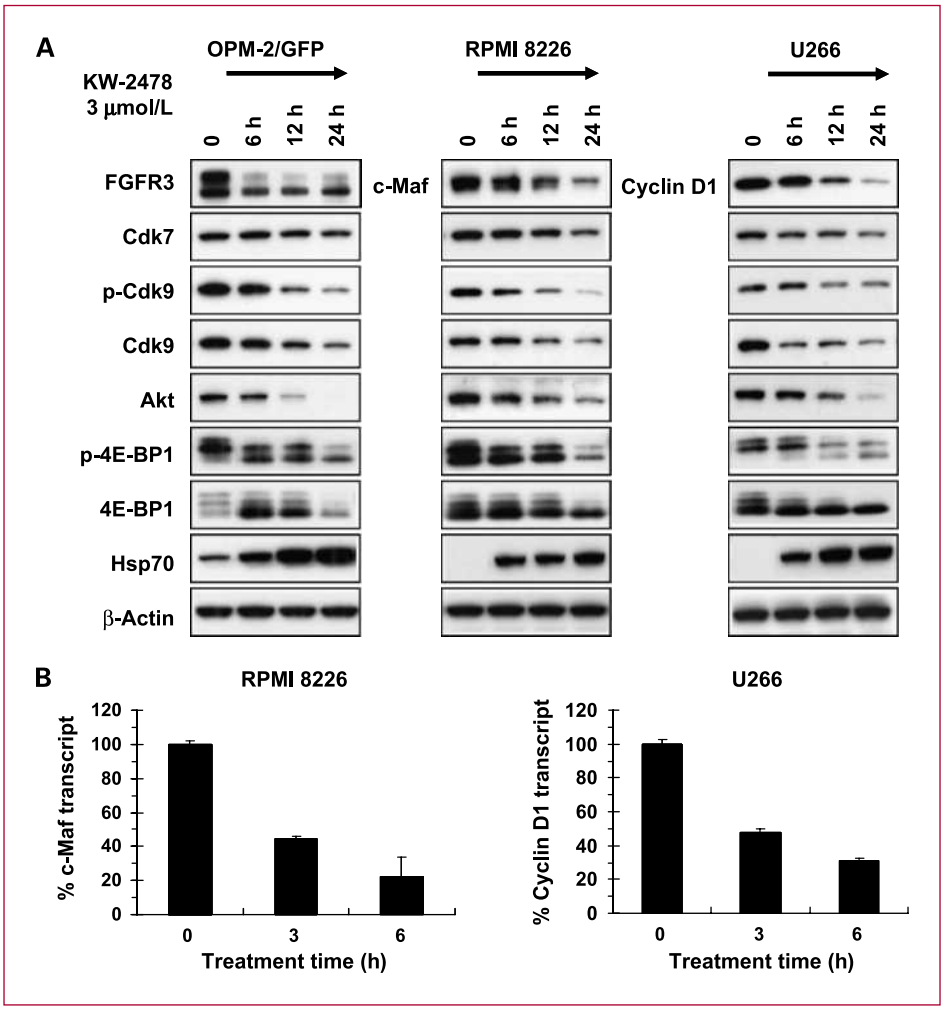

Fig. 4. Time dependent effects of KW-2478 on the IgH translocation products. A, OPM-2/GFP, RPMI 8226, and U266 cells were treated with KW-2478 (3 μmol/L) for 6, 12, and 24 h. Whole-cell lysates were analyzed by Western blot analysis with FGFR3, c-Maf, cyclin D1, Cdk7, phosphorylated Cdk9 (Thr^{186}), Cdk9, Akt, phosphorylated 4E-BP1 ($Thr^{37/46}$), 4E-BP1, Hsp70, and β-actin antibodies. B, RPMI 8226 and U266 cells were treated with KW-2478 (3 μmol/L) for 3 or 6 h. Real-time PCR was done on cDNA prepared from the cells after drug treatment. The levels of c-Maf and cyclin D1 mRNA were determined. After normalizing to glyceraldehyde-3-phosphate dehydrogenase mRNA, the relative levels were expressed as percentage of control. Column, mean; bras, SD ($n = 2$).

the fluorescence in KW-2478–treated mice was clearly reduced compared with that in the control mice (Fig. 6B). In addition, serum M protein concentrations in the tumor-bearing mice were also measured, because the concentration of M protein is used for diagnosis and determination of clinical response in MM patients. When the concentrations of serum M protein were measured on days 31, 38, and 45, statistically significant decreases in serum M protein were detected in KW-2478–treated mice (Fig. 6C). This finding was consistent with the WFI observations of each mouse on day 48. These results indicate that KW-2478 exerted an antitumor activity against MM tumors growing in the bone marrow. In these *in vivo* experiments, KW-2478 was well tolerated and no severe toxicity was observed as assessed by treatment-related mortality and body weight change.

Discussion

Hsp90 assists the correct conformation, stabilization, and activation of its client proteins, most of which are responsible for the oncogenic addiction of various tumors. In addition, Hsp90 contributes to oncogenesis as the nononcogenic addiction, managing various cellular stresses (e.g., hypoxic, metabolic, oxidative, or proteotoxic stress) in cancer cells (5, 33, 34). In this study, we reported the pharmacologic profile of a novel Hsp90 inhibitor, KW-2478. Due to its good solubility in saline (>30 mg/mL), no hepatotoxicity in animal studies (data not shown), acceptable pharmacokinetic profile, and no metabolism by CYP3A4 enzyme (data not shown), KW-2478 might overcome limitation of geldanamycin analogues.

The previous reports have revealed that inhibition of Hsp90 function with the Hsp90 inhibitors (e.g., 17-AAG and NVP-AUY922) or siRNA-mediated silencing leads to growth arrest and apoptosis in MM cell lines and primary MM cells (15, 16, 35). A pronounced feature of Hsp90 inhibition in MM cells is suppression of cell surface expression of interleukin-6R, IGF-IRβ, and their downstream signaling molecules (signal transducers and activators of transcription 3, Erk1/2, and NF-κB; refs. 15, 16, 35). However, little is known about the effects of Hsp90 inhibitors on the chromosomal translocation products (e.g., FGFR3,

c-Maf, and cyclin D1) on the IgH locus that caused the development of the disease.

In this study, we discovered that KW-2478 induced depletion of the FGFR3 protein, in OPM-2/GFP and NCI-H929 cells, indicating that FGFR3 could be a new Hsp90 client protein (Figs. 2B and 4A; Supplementary Figs. S2 and S3). Furthermore, KW-2478 decreased the levels of c-Maf and cyclin D1 proteins at the concentrations that induced the depletion of Hsp90 client proteins in each cell line (Fig. 2B). When we examined the phosphorylation status of various signaling molecules (Erk1/2, Akt, Cdk9, and 4E-BP1), the phosphorylated Cdk9 (Thr^{186}) and phosphorylated 4E-BP1 ($Thr^{37/46}$) were clearly detected in all MM cell lines, indicating that these molecules might play critical roles in the excess expression of IgH translocation products (Supplementary Fig. S4).

Several groups have reported that the transcriptional Cdks (Cdk7, Cdk9) phosphorylate the carboxy-terminal RNA polymerase II, facilitating transcriptional initiation and elongation, which affect the transcripts with short half-lives (e.g., Mcl-1; ref. 36, 37). It is also reported that Cdk9 inhibitors (e.g., flavopiridol) suppress the transcription of Mcl-1 in hematologic tumor cells (38, 39). When we analyzed the protein level of Cdk9 after KW-2478 treatment, we confirmed its time-dependent downregulation in MM cells, preceding the decrease of c-Maf and cyclin D1 (Fig. 4A). To clarify the mechanism of action for these results, we examined the transcripts of c-Maf in RPMI 8226

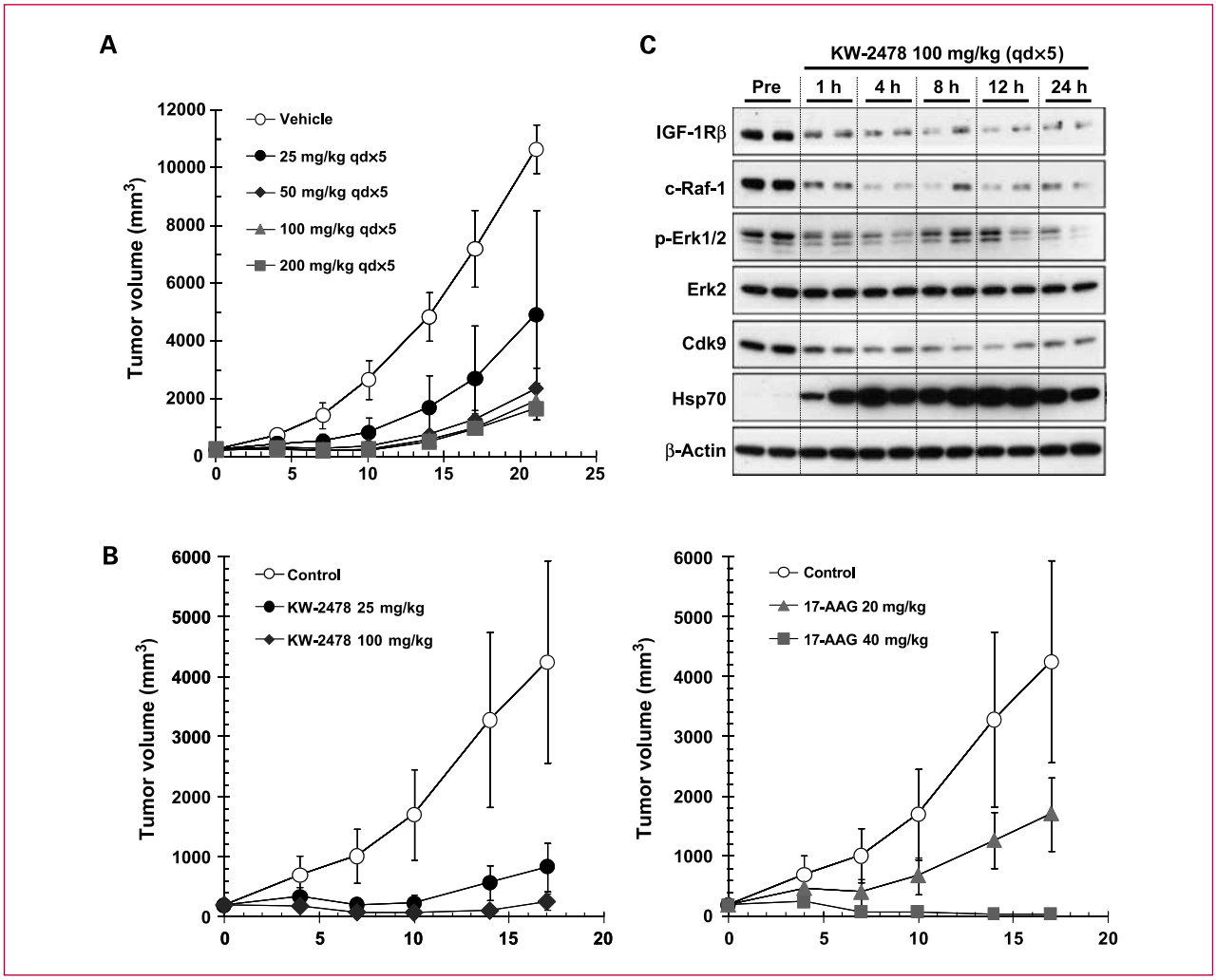

Fig. 5. Effects of KW-2478 in NCI-H929 tumors s.c. inoculated in SCID mice. A, SCID mice with NCI-H929 tumors were prepared. After randomly grouping (five mice per group), saline (vehicle control) or KW-2478 (25, 50, 100, and 200 mg/kg) was i.v. given to mice once daily for 5 d (qd x 5). Points, mean; bars, SD. B, SCID mice with NCI-H929 tumors were prepared. After randomly grouping (five mice per group), saline (vehicle control), KW-2478 (25 and 100 mg/kg), or 17-AAG (20 and 40 mg/kg) was i.v. given to mice twice daily for 5 d. Tumor volumes were measured twice weekly. Points, mean; bars, SD. C, molecular changes in tumor induced by KW-2478 dosing. KW-2478 (100 mg/kg) was i.v. given to mice bearing s.c. NCI-H929 tumors once daily for 5 d (qd × 5). At 1, 4, 8, 12, and 24 h after the fifth administration, tumor samples were collected. Hsp90 client proteins (IGF-IRβ, c-Raf-1, and Cdk9), phosphorylated Erk1/2 (Thr^{202}/Tyr^{204}), and Hsp70 levels in tumors were examined by Western blot analysis. Each lane represents an individual tumor sample.

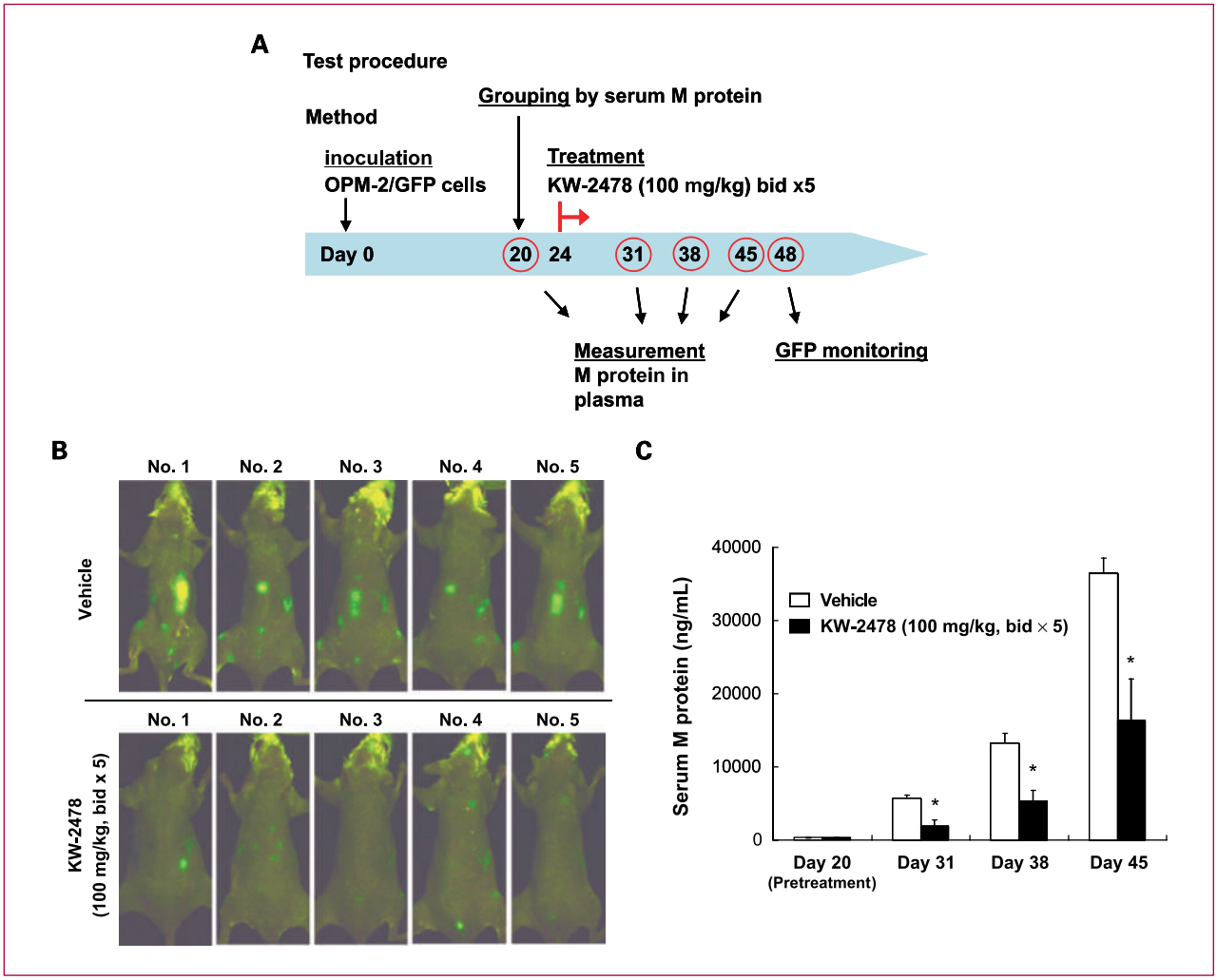

Fig. 6. *In vivo* antitumor activity of KW-2478 in MM orthotopic model. A, test procedure of MM orthotopic model. SCID mice were i.v. inoculated with human OPM-2 cells stably transfected with a GFP gene (OPM-2/GFP) on day 0. Twenty-four days after inoculation of OPM-2/GFP cells, KW-2478 (100 mg/kg) was given i.v. twice daily for 5 d (bid × 5). B, on day 48 (20 d after the end of the administration period), the whole-body fluorescence of each mouse was measured. C, on days 20, 31, 38, and 45 (before drug administration and 3, 10, and 17 d after the end of drug administration, respectively), serum M protein (Ig λ chain) concentrations of the tumor-bearing mice were measured. For statistical analysis of serum M protein concentration, Wilcoxon rank-sum test was done using the SAS software (*, $P < 0.05$, significant). Column, mean; bars, SD ($n = 5$).

and cyclin D1 in U266 cells treated with KW-2478. As a result, KW-2478 decreased c-Maf and cyclin D1 mRNAs from 3 hours after drug exposure, which suggested the downregulation of Cdk9 by KW-2478 could reduce these transcripts (Fig. 4B). In addition, we found that a well-known Cdk9 inhibitor, flavopiridol, also reduced the level of c-Maf in RPMI 8226 and cyclin D1 in U266 cells without affecting β-actin (Supplementary Fig. S5). Regarding the translational pathway, phosphorylated 4E-BP1 was examined. 4E-BP1 has been extensively studied as a translation inhibitor that binds to eIF4E and blocks its normal function of recruiting the translational initiation complex. However, the phosphorylation of 4E-BP1 by several kinases (e.g., mammalian target of rapamycin) frees eIF4E and stimulates protein synthesis (32). Our data showed that KW-2478 induced the pronounced dephosphorylation of 4E-BP1 in a time-dependent manner, preceding the decrease of c-Maf and cyclin D1 (Fig. 4A). These results revealed that both inhibitory effects of KW-2478 on the Cdk9-mediated transcriptional pathway as well as the 4E-BP1–regulated translational pathway could be critical events for the suppression of IgH translocation products.

When we examined time dependency of antiproliferative activity in OPM-2/GFP and NCI-H929 cells, exposure to KW-2478 for >12 hours showed potent antiproliferative activity (Fig. 3). In addition, time course analysis of Western blotting indicated that 12 hours of exposure to KW-2478 induced significant depletion of various client proteins (FGFR3, Cdk9, and Akt) as well as eventual downregulation of signaling molecules, whereas 6 hours of exposure induced slight or little effects on the expression of these molecules (Fig. 4A). These data indicated that

growth inhibitory activity of KW-2478 is dependent on the downregulation of Hsp90 client proteins and its exposure time. Taken together, our results showed that the depletion of Hsp90 client proteins induced by continuous exposure to KW-2478 caused irreversible growth inhibition and apoptosis in MM cells.

The *in vivo* antitumor activity of KW-2478 was examined in a SCID mouse bearing NCI-H929 xenograft. In this model, i.v. administration of KW-2478 once daily for 5 days showed significant suppression of tumor growth and tumor regressions at doses of 100 mg/kg or more (Fig. 5A). In addition, the molecular changes in tumors were examined after KW-2478 treatment. KW-2478 induced obvious induction of Hsp70 and clear reduction of IGF-IRβ, c-Raf-1, Cdk9, and phosphorylated Erk1/2 in NCI-H929 tumors (Fig. 5C). These results revealed that the degradation of the Hsp90 client proteins in tumors, proof of pharmacologic activities, was responsible for its antitumor activity. Moreover, in this model, we found that KW-2478 shows wider therapeutic index than 17-AAG (Fig. 5B). The daily administration of KW-2478 was feasible in mice without apparent toxicity compared with 17-AAG. In clinical trials, the daily administration of 17-AAG has been limited by formulation difficulties and hepatotoxicity derived from its quinone moiety. Although the intermittent dosing of 17-AAG might be sufficient to somewhat show clinical activity in patients, the intermittent dosing is likely much less effective against some tumors than the frequent dosing. In animal studies, no hepatotoxicity was observed after intensive daily dosing of KW-2478 even at the maximum tolerated dose (data not shown). Therefore, these data suggested that KW-2478, a nonansamycin Hsp90 inhibitor, could overcome the toxicity profile by 17-AAG.

Recent reports have described the developments of some orthotopic MM models in mice, using MM cells stably expressing luciferase or GFP (40, 41). In this novel orthotopic model, we confirmed OPM-2/GFP cell penetration into the bone marrow space of mice developing the disease by immunohistochemical analyses (data not shown). The ability of OPM-2/GFP cells to preferentially grow in the bone marrow environment was consistent with the pathologic condition in MM disease. These observations suggest that this model has provided a useful tool for pharmacologic evaluation of MM therapy. In this model, KW-2478 exerted an antitumor activity against MM tumors growing in the bone marrow environment, correlated with a decrease in M protein (Fig. 6B and C). The results from this study provided a pharmacologically relevant rationale for clinical development of KW-2478 in MM patients. In this report, we focused on the potential use of KW-2478 against MM as the monotherapeutic agent. We have recently shown that the combination of KW-2478 and bortezomib, a proteasome inhibitor, has synergistic effects both *in vitro* and *in vivo*, indicating that KW-2478 could also be a useful drug in combination with bortezomib (in preparation for next publication).

In summary, we reported the molecular and biological effects of a novel Hsp90 inhibitor, KW-2478. This compound bound to Hsp90α with high affinity and inhibited the growth of various hematologic tumor cells. In this study, we showed a new Hsp90 client protein, FGFR3, as well as new mechanism of action by an Hsp90 inhibitor. Exposure of KW-2478 to MM cells not only depleted well-known Hsp90 client proteins but also IgH translocation products (cyclin D1 and c-Maf). We confirmed that the depletion of Cdk9 and the dephosphorylation of 4E-BP1 could be critical for the downregulation of c-Maf and cyclin D1. Moreover, we showed that KW-2478 inhibits *in vivo* s.c. tumor growth of NCI-H929 and i.v. inoculated OPM-2/GFP cells growing in the bone marrow. In addition to the degradation of Hsp90 client proteins, targeting such diverse pathways by the Hsp90 inhibitor could be a promising strategy for the treatment of MM, characterized by complex cytogenetic abnormalities, such as IgH chromosomal translocations. KW-2478 is under clinical investigation in MM patients.

Disclosure of Potential Conflicts of Interest

All the authors are employed by Kyowa Hakko Kirin Co., Ltd.

Acknowledgments

We thank K. Koshimura, M. Asano, K. Higuchi, and K. Nakajima for their technical assistance and A. Shudo and T. Akiyama for their critical reading of the manuscript and helpful discussion.

The costs of publication of this article were defrayed in part by the payment of page charges. This article must therefore be hereby marked *advertisement* in accordance with 18 U.S.C. Section 1734 solely to indicate this fact.

Received 11/24/2009; revised 03/07/2010; accepted 03/29/2010; published OnlineFirst 05/04/2010.

References

1. Kyle RA, Rajkumar SV. Multiple myeloma. N Engl J Med 2004;351:1860–73.
2. Hideshima T, Mitsiades C, Tonon G, Richardson PG, Anderson KC. Understanding multiple myeloma pathogenesis in the bone marrow to identify new therapeutic targets. Nat Rev Cancer 2007;7:585–98.
3. Agnelli L, Bicciato S, Mattioli M, et al. Molecular classification of multiple myeloma: a distinct transcriptional profile characterizes patients expressing CCND1 and negative for 14q32 translocations. J Clin Oncol 2005;23:7296–306.
4. Whitesell L, Lindquist SL. HSP90 and the chaperoning of cancer. Nat Rev Cancer 2005;5:761–72.
5. Neckers L. Heat shock protein 90: the cancer chaperone. J Biosci 2007;32:517–30.
6. Whitesell L, Mimnaugh EG, De Costa B, Myers CE, Neckers LM. Inhibition of heat shock protein HSP90–60v-src heteroprotein complex formation by benzoquinone ansamycins: essential role for stress proteins in oncogenic transformation. Proc Natl Acad Sci U S A 1994;91:8324–8.

7. Soga S, Kozawa T, Narumi H, et al. Radicicol leads to selective depletion of Raf kinase and disrupts K-Ras-activated aberrant signaling pathway. J Biol Chem 1998;273:822–8.
8. Soga S, Neckers LM, Schulte TW, et al. KF25706, a novel oxime derivative of radicicol, exhibits *in vivo* antitumor activity via selective depletion of Hsp90 binding signaling molecules. Cancer Res 1999; 59:2931–8.
9. Shiotsu Y, Neckers LM, Wortman I, et al. Novel oxime derivatives of radicicol induce erythroid differentiation associated with preferential G(1) phase accumulation against chronic myelogenous leukemia cells through destabilization of Bcr-Abl with Hsp90 complex. Blood 2000;96:2284–91.
10. Hostein I, Robertson D, DiStefano F, Workman P, Clarke PA. Inhibition of signal transduction by the Hsp90 inhibitor 17-allylamino-17-demethoxygeldanamycin results in cytostasis and apoptosis. Cancer Res 2001;61:4003–9.
11. Solit DB, Zheng FF, Drobnjak M, et al. 17-Allylamino-17-demethoxygeldanamycin induces the degradation of androgen receptor and HER-2/neu and inhibits the growth of prostate cancer xenografts. Clin Cancer Res 2002;8:986–93.
12. Solit DB, Basso AD, Olshen AB, Scher HI, Rosen N. Inhibition of heat shock protein 90 function down-regulates Akt kinase and sensitizes tumors to Taxol. Cancer Res 2003;63:2139–44.
13. Sausville EA, Tomaszewski JE, Ivy P. Clinical development of 17-allylamino, 17-demethoxygeldanamycin. Curr Cancer Drug Targets 2003;3:377–83.
14. Solit DB, Chiosis G. Development and application of Hsp90 inhibitors. Drug Discov Today 2008;13:38–43.
15. Mitsiades CS, Mitsiades NS, McMullan CJ, et al. Antimyeloma activity of heat shock protein-90 inhibition. Blood 2006;107:1092–100.
16. Chatterjee M, Jain S, Stühmer T, et al. STAT3 and MAPK signaling maintain overexpression of heat shock proteins 90α and β in multiple myeloma cells, which critically contribute to tumor-cell survival. Blood 2007;109:720–8.
17. Mitsiades C, Richardson P, Chanan-Khan A, et al. Phase 1 trial of 17-AAG in patients with relapsed and refractory multiple myeloma (MM). ASCO (American Society of Clinical Oncology) Annual Meeting 2005;Abstract No. 3056.
18. Richardson PG, Chanan-Khan AA, Alsina M, et al. Safety and activity of KOS-953 in patients with relapsed refractory multiple myeloma (MM): Interim results of a phase 1 trial. Blood (ASH Annual Meeting Abstracts) 2005;106:Abstract No. 361.
19. Egorin MJ, Rosen DM, Wolff JH, Callery PS, Musser SM, Eiseman JL. Metabolism of 17-(allylamino)-17-demethoxygeldanamycin (NSC 330507) by murine and human hepatic preparations. Cancer Res 1998;58:2385–96.
20. Kelland LR, Sharp SY, Rogers PM, Myers TG, Workman P. DT-Diaphorase expression and tumor cell sensitivity to 17-allylamino, 17-demethoxygeldanamycin, an inhibitor of heat shock protein 90. J Natl Cancer Inst 1999;91:1940–9.
21. Eccles SA, Massey A, Raynaud FI, et al. NVP-AUY922: a novel heat shock protein 90 inhibitor active against xenograft tumor growth, angiogenesis, and metastasis. Cancer Res 2008;68:2850–60.
22. Karapanagiotou EM, Syrigos K, Saif MW. Heat shock protein inhibitors and vaccines as new agents in cancer treatment. Expert Opin Investig Drugs 2009;18:161–74.
23. Agatsuma T, Ogawa H, Akasaka K, et al. Halohydrin and oxime derivatives of radicicol: synthesis and antitumor activities. Bioorg Med Chem 2002;10:3445–54.
24. Nakashima T, Tanaka R, Yamashita Y, Kanda Y, Hara M. Aranorosin and a novel derivative inhibit the anti-apoptotic functions regulated by Bcl-2. Biochem Biophys Res Commun 2008;377:1085–90.
25. Gazdar AF, Oie HK, Kirsch IR, Hollis GF. Establishment and characterization of a human plasma cell myeloma culture having a rearranged cellular myc proto-oncogene. Blood 1986;67:1542–9.
26. Katagiri S, Yonezawa T, Kuyama J, et al. Two distinct human myeloma cell lines originating from one patient with myeloma. Int J Cancer 1985;36:241–6.
27. Lang SA, Moser C, Gaumann A, et al. Targeting heat shock protein 90 in pancreatic cancer impairs insulin-like growth factor-I receptor signaling, disrupts an interleukin-6/signal-transducer and activator of transcription 3/hypoxia-inducible factor-1α autocrine loop, and reduces orthotopic tumor growth. Clin Cancer Res 2007;13:6459–68.
28. Ronchetti D, Greco A, Compasso S, et al. Deregulated FGFR3 mutants in multiple myeloma cell lines with t(4;14): comparative analysis of Y373C, K650E and the novel G384D mutations. Oncogene 2001;20:3553–62.
29. Shou Y, Martelli ML, Gabrea A, et al. Diverse karyotypic abnormalities of the c-myc locus associated with c-myc dysregulation and tumor progression in multiple myeloma. Proc Natl Acad Sci U S A 2000;97:228–33.
30. Lombardi L, Poretti G, Mattioli M, et al. Molecular characterization of human multiple myeloma cell lines by integrative genomics: insights into the biology of the disease. Genes Chromosomes Cancer 2007; 46:226–38.
31. O'Keeffe B, Fong Y, Chen D, Zhou S, Zhou Q. Requirement for a kinase-specific chaperone pathway in the production of a Cdk9/cyclin T1 heterodimer responsible for P-TEFb-mediated tat stimulation of HIV-1 transcription. J Biol Chem 2000;275:279–87.
32. Armengol G, Rojo F, Castellví J, et al. 4E-binding protein 1: a key molecular "funnel factor" in human cancer with clinical implications. Cancer Res 2007;67:7551–5.
33. Calderwood SK, Khaleque MA, Sawyer DB, Ciocca DR. Heat shock proteins in cancer: chaperones of tumorigenesis. Trends Biochem Sci 2006;31:164–72.
34. Luo J, Solimini NL, Elledge SJ. Principles of cancer therapy: oncogene and non-oncogene addiction. Cell 2009;136:823–37.
35. Stühmer T, Zöllinger A, Siegmund D, et al. Signalling profile and antitumour activity of the novel Hsp90 inhibitor NVP-AUY922 in multiple myeloma. Leukemia 2008;22:1604–12.
36. Shapiro GI. Cyclin-dependent kinase pathways as targets for cancer treatment. J Clin Oncol 2006;24:1770–83.
37. Wang S, Fischer PM. Cyclin-dependent kinase 9: a key transcriptional regulator and potential drug target in oncology, virology and cardiology. Trends Pharmacol Sci 2008;29:302–13.
38. Chen R, Keating MJ, Gandhi V, Plunkett W. Transcription inhibition by flavopiridol: mechanism of chronic lymphocytic leukemia cell death. Blood 2005;106:2513–9.
39. MacCallum DE, Melville J, Frame S, et al. Seliciclib (CYC202, R-Roscovitine) induces cell death in multiple myeloma cells by inhibition of RNA polymerase II-dependent transcription and down-regulation of Mcl-1. Cancer Res 2005;65:5399–407.
40. Mitsiades CS, Mitsiades NS, Bronson RT, et al. Fluorescence imaging of multiple myeloma cells in a clinically relevant SCID/NOD *in vivo* model: biologic and clinical implications. Cancer Res 2003;63:6689–96.
41. Xin X, Abrams TJ, Hollenbach PW, et al. CHIR-258 is efficacious in a newly developed fibroblast growth factor receptor 3-expressing orthotopic multiple myeloma model in mice. Clin Cancer Res 2008; 14:2075–81.